PROCEEDINGS OF SPIE

Fifteenth International Conference on Correlation Optics

Oleg V. Angelsky
Editor

13–16 September 2021
Chernivtsi, Ukraine

Organized by
Chernivtsi National University (Ukraine)

Co-organized by
Research Institute of Zhejiang University-Taizhou (China)

Sponsored by
ICO – International Commission for Optics
Optica (formerly OSA), the Society Advancing Optics and Photonics Worldwide
Frontiers in Physics LTD
LTD "ROMA"
SKB "ELEKTRONMASH" (Ukraine)
Private Clinic of Eye Microsurgery "Your Vision" (Ukraine)
ARTON Company (Ukraine)

Co-sponsored by
SPIE

Published by
SPIE

Volume 12126

Proceedings of SPIE 0277-786X, V. 12126

SPIE is an international society advancing an interdisciplinary approach to the science and application of light.

Fifteenth International Conference on Correlation Optics, edited by Oleg V. Angelsky, Proc. of SPIE Vol. 12126, 1212601
 · 0277-786X · doi: 10.1117/12.2626737

The papers in this volume were part of the technical conference cited on the cover and title page. Papers were selected and subject to review by the editors and conference program committee. Some conference presentations may not be available for publication. Additional papers and presentation recordings may be available online in the SPIE Digital Library at SPIEDigitalLibrary.org.

The papers reflect the work and thoughts of the authors and are published herein as submitted. The publisher is not responsible for the validity of the information or for any outcomes resulting from reliance thereon.

Please use the following format to cite material from these proceedings:
Author(s), "Title of Paper," in *Fifteenth International Conference on Correlation Optics*, edited by Oleg V. Angelsky, Proc. of SPIE 12126, Seven-digit Article CID Number (DD/MM/YYYY); (DOI URL).

ISSN: 0277-786X
ISSN: 1996-756X (electronic)

ISBN: 9781510651289
ISBN: 9781510651296 (electronic)

Published by
SPIE
P.O. Box 10, Bellingham, Washington 98227-0010 USA
Telephone +1 360 676 3290 (Pacific Time)
SPIE.org

Printed in the United States of America by Curran Associates, Inc., under license from SPIE.

Publication of record for individual papers is online in the SPIE Digital Library.

SPIE. DIGITAL LIBRARY
SPIEDigitalLibrary.org

Paper Numbering: A unique citation identifier (CID) number is assigned to each article in the Proceedings of SPIE at the time of publication. Utilization of CIDs allows articles to be fully citable as soon as they are published online, and connects the same identifier to all online and print versions of the publication. SPIE uses a seven-digit CID article numbering system structured as follows:

- The first five digits correspond to the SPIE volume number.
- The last two digits indicate publication order within the volume using a Base 36 numbering system employing both numerals and letters. These two-number sets start with 00, 01, 02, 03, 04, 05, 06, 07, 08, 09, 0A, 0B … 0Z, followed by 10-1Z, 20-2Z, etc. The CID Number appears on each page of the manuscript.

Laser-induced 3D Mueller-matrix microscopy method for forensic evaluation cerebral infarction, hemorrhagic hemorrhages of traumatic genesis

Garazdyuk[1] M.S., Bachinsky[1] V.T., Hulei[1] L, Ushenko[2] V.A.,
Slyotov[2] M., Fesiv[2] I.V. Drin[2] I.I., Drin[2] S.S.

[1] Bukovinian State Medical University, Chernivtsi, Ukraine
[2]Chernivtsi National University, Chernivtsi, Ukraine

ABSTRACT

The paper presents the structural-logical diagram and research design of the newest method of 3D Mueller-matrix microscopy of the layer-by-layer structure of the polycrystalline component [1-9] of depolarizing histological sections of the brain. Principles of differential diagnosis of the formation of hemorrhages of traumatic genesis, cerebral infarction ischemic and hemorrhagic genesis by the method of 3D Mueller-matrix microscopy. Layer-by-layer azimuthal-invariant Mueller-matrix images of circular birefringence (MMI OA) of histological brain sections and operational characteristics of the method of their statistical analysis were determined.

Keywords: polarization, optical anisotropy, linear and circular birefringence, Mueller matrix, statistical moments of the 1st-4th orders, hemorrhages of traumatic genesis, cerebral infarction of ischemic and hemorrhagic genesis

1. STRUCTURAL AND LOGICAL DIAGRAM OF 3D MUELLER-MATRIX MICROSCOPY OF HISTOLOGICAL SECTIONS OF THE BRAIN

<table>
<tr><td colspan="4">Histological sections of the brain of the deceased</td></tr>
<tr><td>Control group deceased (group 1)</td><td>Hemorrhage of traumatic genesis (group 2)</td><td>Cerebral infarction of ischemic genesis (group 3)</td><td>Cerebral infarction of hemorrhagic genesis (group 4)</td></tr>
<tr><td colspan="4">3D Mueller-matrix mapping</td></tr>
<tr><td colspan="4">Layered maps of optical activity (circular birefringence) (MMI OA)</td></tr>
<tr><td colspan="4">Statistical Analysis of Layered Maps MMI OA</td></tr>
<tr><td colspan="4">Average values and standard deviations of the magnitude of the statistical moments of the 1st - 4th orders, which characterize the coordinate distributions MMI OA</td></tr>
<tr><td colspan="4">Criteria for differential diagnosis of samples of histological sections of the brain of the deceased from groups 1 - 4</td></tr>
</table>

Fig. 1. Structural and logical diagram of 3D Mueller-matrix microscopy of histological sections of the brain

2. DIFFERENTIAL DIAGNOSIS OF THE FORMATION OF HEMORRHAGES OF TRAUMATIC GENESIS, CEREBRAL INFARCTION OF ISCHEMIC AND HEMORRHAGIC GENESIS BY THE METHOD OF 3D MUELLER-MATRIX MICROSCOPY

The results of the study of the layer-by-layer coordinate distributions of the value of the Mueller-matrix invariant of circular birefringence (MMI OA) of the protein complexes [10-13] of the nervous tissue of histological sections of the brain of the deceased from different groups by the method of 3D Mueller-matrix microscopy are shown on a series of fragments in Fig. 2 - Fig. 4.

Fifteenth International Conference on Correlation Optics, edited by Oleg V. Angelsky, Proc. of SPIE Vol. 12126, 121262A
© 2021 SPIE · 0277-786X · doi: 10.1117/12.2616838

We used the following phase sections of 3D distributions of the field of complex amplitudes for digital holographic reproduction of MMI OA:

- $\delta = 0{,}4rad$ - practically single scattering;
- $\delta = 0{,}8rad$ - scattering of medium multiplicity;
- $\delta = 1{,}2rad$ - multiple scattering in the volume of a real sample.

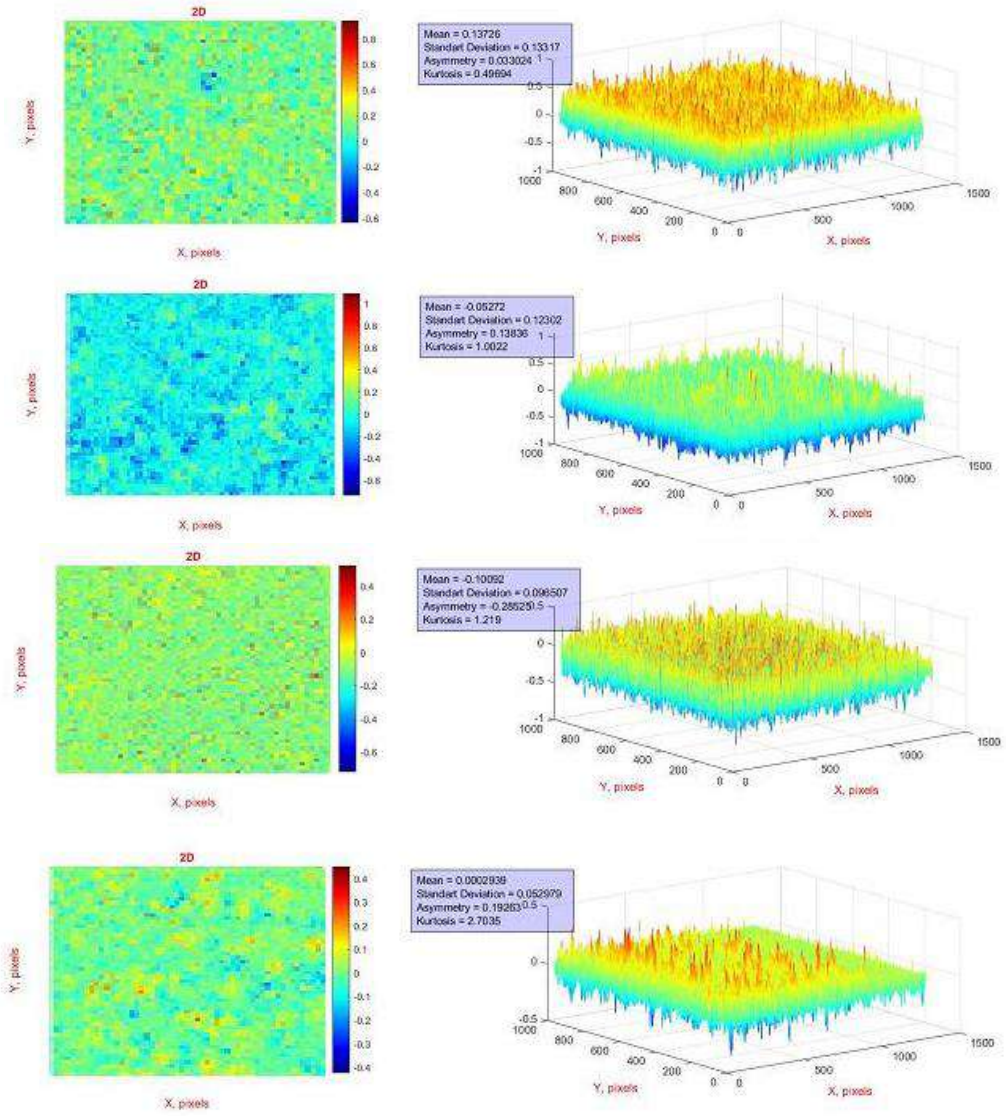

Fig. 2. Maps ((1), (2), (3), (4)) and histograms ((4), (5), (6), (7)) of the distribution of the value of MMI OA of histological brain sections of the deceased from group 1 ((1), (5)), group 2 ((2), (6)), group 3 ((3), (7)) and group 4 ((4), (8)) for the phase section $\delta = 0{,}4rad$.

From analysis of the obtained data of 3D Mueller-matrix mapping of layer-by-layer polarization manifestations [14-21] of optical activity of a set of histological brain sections for cases of coronary heart disease (group 1), traumatic hemorrhage (group 2), cerebral infarction of hemorrhagic (group 3) and ischemic (group 4) genesis was established:

1. Phase section $\delta = 0{,}4\text{rad}$:

- individual topographic structure of all MMI OA maps of a given phase section of the optically anisotropic component of histological sections of the brain nervous tissue of the deceased from all groups (Fig. 2, fragments (1), (3), (5), (7));
- The histograms characterizing the distributions of the optical activity of brain samples from all (control 1 and research 2-4) groups are characterized by significant average values SM_1 and scatter of values (dispersion SM_2), large skewness (SM_3) and kurtosis SM_4 (Fig. 2, fragments (2) (4), (6), (8));

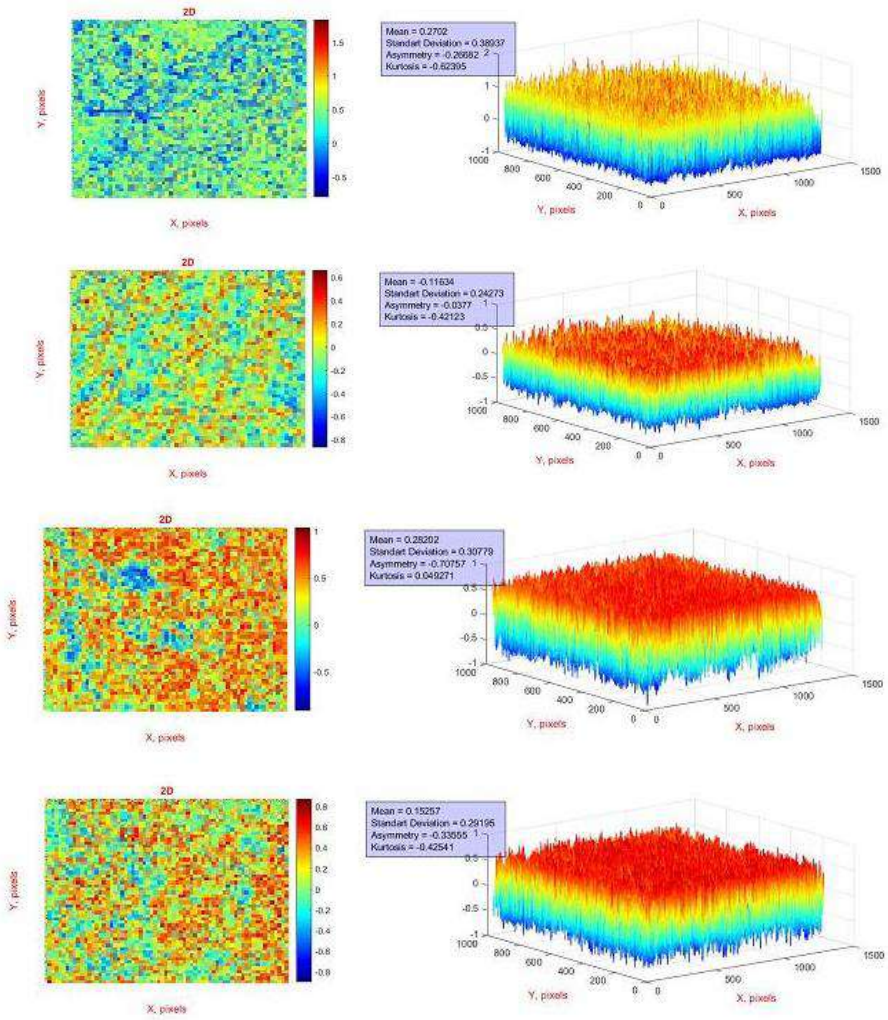

Fig. 3. Maps ((1), (2), (3), (4)) and histograms ((4), (5), (6), (7)) of the distribution of the value of MMI OA of histological brain sections of the deceased from group 1 ((1), (5)), group 2 ((2), (6)), group 3 ((3), (7)) and group 4 ((4), (8)) for the phase section $\delta = 0{,}8rad$.

2. Phase section $\delta = 0{,}8\text{rad}$:

- a more homogeneous, compared with the results of 3D Mueller-matrix polarimetry of the distributions of the circular birefringence value of the optically thin phase plane ($\delta = 0{,}4rad$), the topological structure of MMI OA, which

characterizes circularly birefringent protein complexes of the nervous tissue of the deceased from all groups (Fig. 3, fragments (1), (3), (5), (7));

- for histograms, characterizing layer-by-layer MMI OA maps in a phase section with an intermediate scattering multiplicity, of samples from all (control 1 and research 2 - 4) groups are characterized by an increase in the scatter of values (dispersion SM_2), and a decrease in the magnitude of skewness (SM_3) and sharpness (kurtosis SM_4) of the peak (Fig. 3, fragments (2), (4), (6), (8));

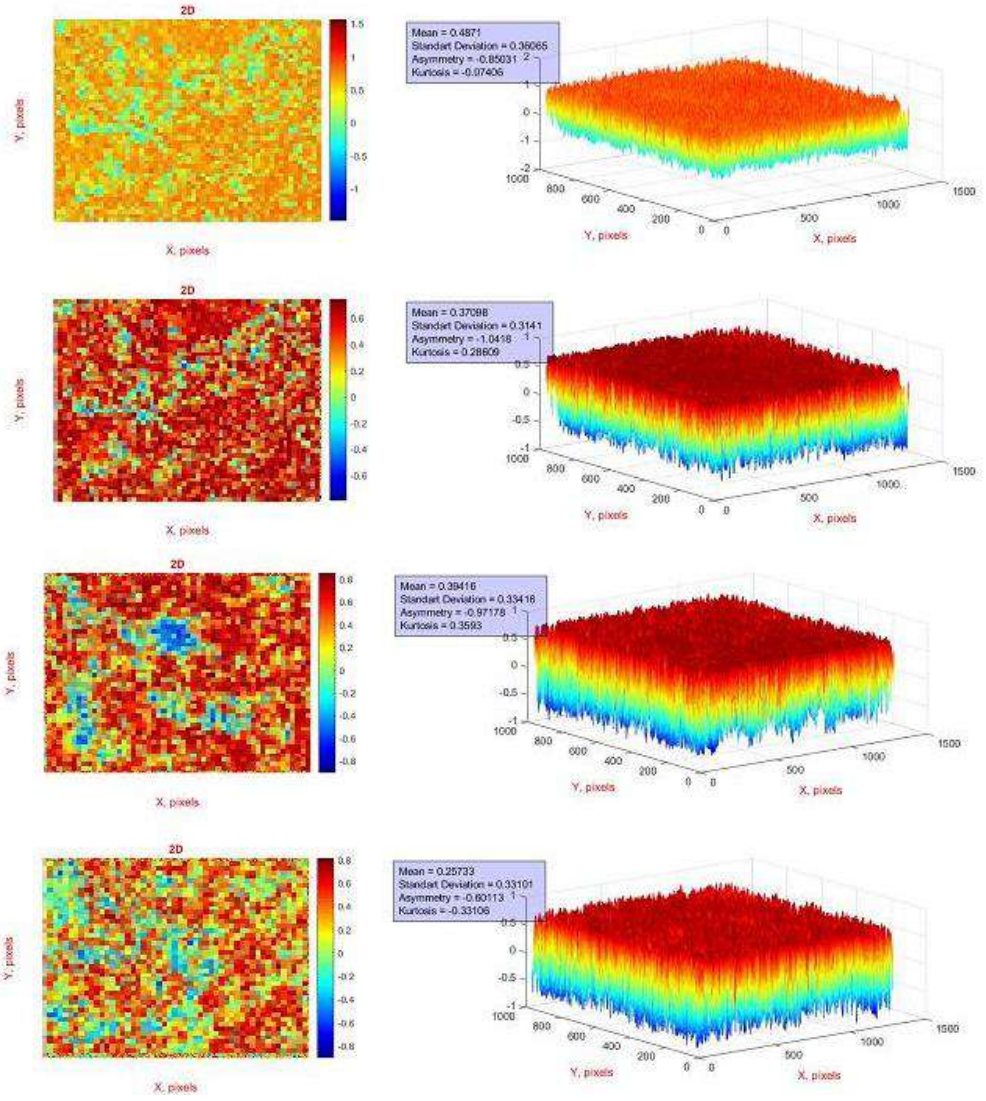

Fig. 4. Maps ((1), (2), (3), (4)) and histograms ((4), (5), (6), (7)) of the distribution of the value of MMI OA of histological brain sections of the deceased from group 1 ((1), (5)), group 2 ((2), (6)), group 3 ((3), (7)) and group 4 ((4), (8)) for the phase section $\delta = 1{,}2 rad$.

3. Phase section $\delta = 1{,}2 \text{rad}$:

- close to the results of the direct Mueller-matrix polarimetry of all integrated maps of MMI OA of histological sections of the nervous tissue of the brain that deceased from all groups, the topological structure of distributions of the

magnitude of circular birefringence in the phase plane, which is formed by multiple scattering of laser radiation over the entire volume of the sample;

- the histograms characterizing the MMI maps of samples from all (control 1 and research 2 - 4) groups are characterized by maximum, but similar in magnitude, average SM_1, scatter of values (dispersion SM_2), minimum skewness SM_3 and kurtosis SM_4 (Fig. 4, fragments (2) (4), (6), (8)).

In a series of tables 1 - 3, the mean values and errors ($\pm\Omega$) of determining the set of statistical moments of the 1st - 4th orders $SM_{i=1-4}$ are presented, which characterize the layered Mueller-matrix images of polarization manifestations of circular birefringence of optically active protein complexes of the nervous tissue of the brain in various phase planes.

Table 1 Statistical moments of the 1st - 4th orders, characterizing the distributions of the MMI OA value of histological sections of the brain of groups 1 - 4 for the phase section $\delta = 0{,}4 rad$

Parameters	Group 1	Group 2	Group 3	Group 4
SM_1	$0{,}28 \pm 0{,}013$	$0{,}21 \pm 0{,}009$	$0{,}17 \pm 0{,}008$	$0{,}14 \pm 0{,}006$
p	$p \prec 0{,}05$			
SM_2	$0{,}31 \pm 0{,}013$	$0{,}25 \pm 0{,}011$	$0{,}21 \pm 0{,}009$	$0{,}16 \pm 0{,}007$
p	$p \prec 0{,}05$			
SM_3	$0{,}87 \pm 0{,}035$	$1{,}12 \pm 0{,}059$	$1{,}57 \pm 0{,}063$	$1{,}98 \pm 0{,}089$
p	$p \prec 0{,}05$			
SM_4	$1{,}88 \pm$	$2{,}56 \pm 0{,}11$	$3{,}09 \pm 0{,}13$	$3{,}89 \pm 0{,}15$
p	$p \prec 0{,}05$			

Table 2 Statistical moments of the 1st - 4th orders, characterizing the distributions of the MMI OA value of histological sections of the brain of groups 1 - 4 for the phase section $\delta = 0{,}8 rad$

Parameters	Group 1	Group 2	Group 3	Group 4
SM_1	$0{,}32 \pm 0{,}012$	$0{,}27 \pm 0{,}011$	$0{,}23 \pm 0{,}0105$	$0{,}19 \pm 0{,}08$
p	$p \prec 0{,}05$			
SM_2	$0{,}36 \pm 0{,}013$	$0{,}32 \pm 0{,}012$	$0{,}28 \pm 0{,}011$	$0{,}24 \pm 0{,}009$
p	$p \prec 0{,}05$			
SM_3	$0{,}68 \pm 0{,}026$	$0{,}82 \pm 0{,}035$	$1{,}05 \pm 0{,}043$	$1{,}29 \pm 0{,}052$
p	$p \prec 0{,}05$			
SM_4	$1{,}18 \pm 0{,}047$	$1{,}45 \pm 0{,}066$	$1{,}89 \pm 0{,}083$	$2{,}28 \pm 0{,}094$
p	$p \prec 0{,}05$			

Table 3 Statistical moments of the 1st - 4th orders, characterizing the distributions of the MMI OA value of histological sections of the brain of groups 1 - 4 for the phase section $\delta = 1,2 rad$

Parameters	Group 1	Group 2	Group 3	Group 4
SM_1	$0,35 \pm 0,016$	$0,32 \pm 0,014$	$0,28 \pm 0,013$	$0,25 \pm 0,012$
p	$p \prec 0,05$			
p	$p \succ 0,05$			
SM_2	$0,38 \pm 0,017$	$0,34 \pm 0,016$	$0,32 \pm 0,015$	$0,29 \pm 0,014$
p	$p \prec 0,05$			
p	$p \succ 0,05$			
SM_3	$0,56 \pm 0,019$	$0,62 \pm 0,023$	$0,75 \pm 0,028$	$0,82 \pm 0,033$
p	$p \prec 0,05$			
p	$p \succ 0,05$			
SM_4	$0,71 \pm 0,028$	$0,84 \pm 0,036$	$1,09 \pm 0,044$	$1,27 \pm 0,058$
p	$p \prec 0,05$			
p	$p \succ 0,05$			

Comparative analysis of the data obtained revealed:

1. Phase section $\delta = 0,4 rad$ (table 1):
   The maximum intergroup differences in the magnitude of the set of statistical moments of the 1st - 4th orders and the statistical significance of differentiation of cases of coronary heart disease (control group 1), traumatic hemorrhage (research group 2), cerebral infarction of ischemic (research group 3) and hemorrhagic (research group 4) genesis.
2. Phase section $\delta = 0,8 rad$ (table 2):
   Significant intergroup differences in mean values within the representative samples of histological sections of the brain, the magnitude of the set of statistical moments of the 1st - 4th orders and the statistical reliability of differentiation of cases from control group 1 and research group 2 - group 4.
3. Phase section $\delta = 1,2 rad$ (table 3):
   the possibility of statistically significant differentiation is realized only between group 1 and groups 2 - 4.

3. OPERATIONAL CHARACTERISTICS OF THE METHOD OF STATISTICAL ANALYSIS OF LAYER-BY-LAYER MMI OA MAPS OF HISTOLOGICAL BRAIN SECTIONS.

The series table 4 - table 6 presents the results of information analysis of determining the strength (balanced accuracy) of the 3D Mueller-matrix mapping method in various phase planes of the distributions of the MMI OA value.

The possibility and effectiveness of differentiation was considered:

- control group 1 – all research groups 2+3+4;
- research group 2 – research group 4;
- research group 2 – research group 3;
- research group 3 – research group 4.

Table 4 Balanced accuracy of the method of statistical analysis of MMI OA maps of histological brain sections for phase section $\delta = 0{,}4 rad$

Parameters	**Balanced accuracy** Ac,%			
Groups	**“1”-“2+3+4”**	**“2”-“4”**	**“2”-“3”**	**“3”-“4”**
SM_1	**86**	**85**	**82**	**80**
SM_2	**88**	**86**	**83**	**82**
SM_3	**96**	**95**	**92**	**85**
SM_4	**96**	**95**	**93**	**86**

Table 5 Balanced accuracy of the method of statistical analysis of MMI OA maps of histological brain sections for phase section $\delta = 0{,}8 rad$

Parameters	**Balanced accuracy** Ac,%			
Groups	**“1”-“2+3+4”**	**“2”-“4”**	**“2”-“3”**	**“3”-“4”**
SM_1	**82**	**78**	**76**	**70**
SM_2	**81**	**76**	**78**	**72**
SM_3	**89**	**88**	**85**	**78**
SM_4	**90**	**87**	**86**	**76**

Table 6 Balanced accuracy of the method of statistical analysis of MMI OA maps of histological brain sections for phase section $\delta = 1{,}2 rad$

Parameters	**Balanced accuracy** Ac,%			
Groups	**“1”-“2+3+4”**	**“2”-“4”**	**“2”-“3”**	**“3”-“4”**
SM_1	**68**	**66**	**64**	**58**
SM_2	**72**	**70**	**68**	**60**
SM_3	**78**	**75**	**75**	**67**
SM_4	**82**	**80**	**76**	**72**

A comparative analysis of the obtained data on the balanced accuracy of differentiation of cases of traumatic hemorrhage, cerebral infarction of hemorrhagic and ischemic genesis by the method of 3D Mueller-matrix mapping MMI OA found:

1. Phase section $\delta = 0{,}4 rad$ (table 4):

The maximum level of balanced accuracy between group differentiation by calculating the statistical moments of the 3rd and 4th order, characterizing the skewness and kurtosis of the distributions of the MMI OA value of histological brain sections:

- “1”-“2+3+4” і “2” - “4” - excellent accuracy (95% - 96%);
- “2” - “3” - good accuracy (92% - 93%);
- “3”-“4” - satisfactory accuracy (85% - 86%).

2. Phase section $\delta = 0{,}8 rad$ (table 5):

Significant decrease (by 10% - 15%) to a satisfactory level of balanced accuracy between group differentiation by calculating the skewness and kurtosis of the distributions of the MMI OA value of histological brain sections:

- “1”-“2+3+4” і “2” - “4” - satisfactory accuracy (89% - 90%);
- “2” - “3” - satisfactory accuracy (85% - 86%);
- “3”-“4” - unsatisfactory accuracy (76% - 78%).

3. Phase section $\delta = 1{,}2\text{rad}$ (table 6):

Critical reduction to an unsatisfactory level of balanced accuracy between group differentiation by calculating the skewness and kurtosis of the distributions of the MMI value of the OA of histological brain sections:

- "1"-"2+3+4" і "2" - "4" - unsatisfactory accuracy (78% - 82%);
- "2" - "3" - unsatisfactory accuracy (75% - 80%);
- "3"-"4" - unsatisfactory accuracy (75% - 76%).

CONCLUSIONS

1. A structural and logical scheme has been developed and the design of the 3D Mueller-matrix mapping method has been experimentally tested to improve the diagnostic capabilities of forensic differentiation of cases of cerebral infarction, hemorrhagic hemorrhages of traumatic genesis and to determine the age of their formation by digital holography and azimuthally invariant Mueller-matrix microscopy.
2. It was found that for each of the phase sections of the volumetric distributions of the field of complex amplitudes, the values of sensitivity $\text{Se},\%$, specificity $\text{Sp},\%$, and balanced accuracy $\text{Ac},\%$ of the statistical analysis of the coordinate distributions of MMI OA have maximum values for small phase shifts, which correspond to the level of single scattering.
3. The maximum level of balanced accuracy between group differentiation was revealed by calculating the statistical moments of the 3rd and 4th order, characterizing the skewness and kurtosis of the distributions of the MMI value of the OA of histological brain sections:

- "1"-"2+3+4" і "2" - "4" - excellent accuracy (95% - 96%);
- "2" - "3" - good accuracy (92% - 93%);
- "3"-"4" - satisfactory accuracy (85% - 86%).

FUNDING

Current research supported by the National Research Foundation of Ukraine (Project 2020.02/0061)

REFERENCES

[1] S. P. Morgan and I. M. Stockford, "Surface-reflection elimination in polarization imaging of superficial tissue," Opt. Lett. 28, 114–116 (2003).
[2] M. Hunter et al., "Tissue self-affinity and polarized light scattering in the Born approximation: a new model for precancer detection," Phys. Rev. Lett. 97(13), 138102 (2006).
[3] P. Shukla et al., "Influence of size parameter and refractive index of the scatterer on polarization-gated optical imaging through turbid media," J. Opt. Soc. Am. A 24, 1704–1713 (2007).
[4] V.M. Turzhitsky et al., "Measuring mucosal blood supply in vivo with a polarization-gating probe," Appl. Opt. 47(32), 6046–6057 (2008).
[5] S. M. Daly and M. J. Leahy, "'Go with the flow:' a review of methods and advancements in blood flow imaging," J. Biophotonics 6(3), 217– 255 (2013).
[6] Y. A. Ushenko, "Diagnostics of structure and physiological state of birefringent biological tissues: statistical, correlation and topological approaches," in Coherent-Domain Optical Methods: Biomedical Diagnostics, Environmental Monitoring and Material Science, 2nd ed., V. V. Tuchin, Ed., pp. 107–148, Springer Reference, Science + Business Media, New York (2013).
[7] A. Pierangelo et al., "Ex vivo characterization of human colon cancer by Mueller polarimetric imaging," Opt. Express 19, 1582–1593 (2011).
[8] G. Purvinis, B. D. Cameron, and D. M. Altrogge, "Noninvasive polarimetric-based glucose monitoring: an in vivo study," J. Diabetes Sci. Technol. 5(2), 380–387 (2011).

[9] A. Doronin and I. Meglinski, “Online object oriented Monte Carlo computational tool for the needs of biomedical optics,” Biomed. Opt. Express 2(9), 2461–2469 (2011).
[10] Trifonyuk, L., Baranowski, W., Ushenko, V., Olar, O., Dubolazov, A., Ushenko, Y., Bodnar, B., Vanchulyak, O., Kushnerik, L., Sakhnovskiy, M. 2D-Mueller-matrix tomography of optically anisotropic polycrystalline networks of biological tissues histological sections (2018) Opto-electronics Review, 26 (3), pp. 252-259.
[11] Trifonyuk, L., Baranovsky, V., Dubolazov, O.V., Ushenko, V.O., Ushenko, O.G., Zhytaryuk, V.G., Prydiy, O.G., Vanchulyak, O. Jones-matrix tomography of biological tissues phase anisotropy in the diagnosis of uterus wall prolapse (2018) Proceedings of SPIE - The International Society for Optical Engineering, 10612, 106121F.
[12] Trifonyuk, L., Dubolazov, O.V., Ushenko, Y.O., Zhytaryuk, V.G., Prydiy, O.G., Grytsyuk, M., Kushnerik, L., Meglinskiy, I., Savka, I.G. New opportunities of differential diagnosis of biological tissues polycrystalline structure using methods of Stokes correlometry mapping of polarization inhomogeneous images(2017) Proceedings of SPIE - The International Society for Optical Engineering, 10396, 103962R.
[13] Angelsky, O.V., Bekshaev, A.Y., Dragan, G.S., Maksimyak, P.P., Zenkova, C.Y., Zheng, J. Structured Light Control and Diagnostics Using Optical Crystals (2021) Frontiers in Physics, 9,715045.
[14] Angelsky, O.V., Maksimyak, P.P. Optical diagnostics of slightly rough surfaces (1992) Applied Optics, 31 (1), pp. 140-143
[15] Angelsky, O.V., Zenkova, C.Y., Hanson, S.G., Zheng, J. Extraordinary Manifestation of Evanescent Wave in Biomedical Application (2020) Frontiers in Physics, 8, 159.
[16] Angelsky, O.V., Bekshaev, A.Y., Hanson, S.G., Zenkova, C.Y., Mokhun, I.I., Jun, Z. Structured Light: Ideas and Concepts (2020) Frontiers in Physics, 8, 114
[17] Dubolazov, O.V., Trifonyuk, L., Marchuk, Y., Ushenko, Y.O., Zhytaryuk, V.G., Prydiy, O.G., Kushnerik, L., Meglinskiy, I. Two-point Stokes vector parameters of object field for diagnosis and differentiation of optically anisotropic biological tissues (2017) Proceedings of SPIE - The International Society for Optical Engineering, 10352, 103520V .
[18] P. Wang, X. Zhang, Y. Xiang, F. Shi, M. Gavryliak, and J. Xu, "Random laser with superscatterers at designable wavelengths," Opt. Express 23, 24407-24415 (2015).
[19] Angelsky, O.V., Ushenko, Y.A., Dubolazov, A.V., Telenha, O.Yu. The interconnection between the coordinate distribution of mueller-matrixes images characteristic values of biological liquid crystals net and the pathological changes of human tissues (2010) Advances in Optical Technologies, 130659 . ..11
[20] Ushenko, A.G. Polarization Correlometry of Angular Structure in the Microrelief Pattern of Rough Surfaces (2002) Optics and Spectroscopy (English translation of Optika i Spektroskopiya), 92 (2), pp. 227-229.
[21] Angelsky, O.V., Maksimyak, P.P., Perun, T.O. Optical correlation method for measuring spatial complexity in optical fields (1993) Optics Letters, 18 (2), pp. 90-92.